



OPEN ACCESS

EDITED BY

David Mascali,
Laboratori Nazionali del Sud (INFN), Italy

REVIEWED BY

Zilong Chang,
Indiana University, United States
Theocharis S. Kosmas,
University of Ioannina, Greece

*CORRESPONDENCE

Changbo Fu,
✉ cbfu@fudan.edu.cn
Wanbing He,
✉ hewanbing@fudan.edu.cn

RECEIVED 10 April 2023

ACCEPTED 17 July 2023

PUBLISHED 28 July 2023

CITATION

Wang Y, Ma Z, Yang Y, Fu C, He W and
Ma Y (2023), Feasibility study of nuclear
excitation by electron capture using an
electron beam ion trap.
Front. Phys. 11:1203401.
doi: 10.3389/fphy.2023.1203401

COPYRIGHT

© 2023 Wang, Ma, Yang, Fu, He and Ma.
This is an open-access article distributed
under the terms of the [Creative
Commons Attribution License \(CC BY\)](#).
The use, distribution or reproduction in
other forums is permitted, provided the
original author(s) and the copyright
owner(s) are credited and that the original
publication in this journal is cited, in
accordance with accepted academic
practice. No use, distribution or
reproduction is permitted which does not
comply with these terms.

Feasibility study of nuclear excitation by electron capture using an electron beam ion trap

Yumiao Wang , Zhiguo Ma, Yi Yang, Changbo Fu *,
Wanbing He * and Yugang Ma

Key Laboratory of Nuclear Physics and Ion-beam Application (Ministry of Education), Institute of Modern Physics, Fudan University, Shanghai, China

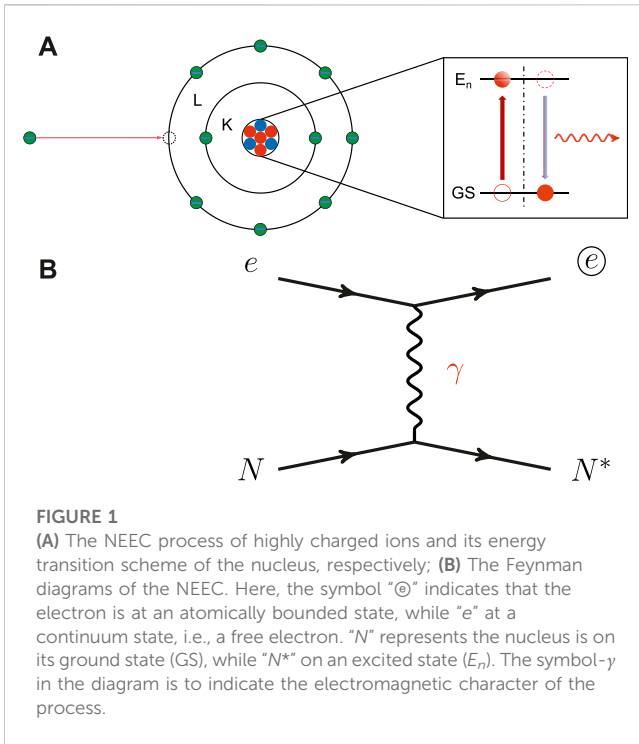
The nuclear excitation by electron capture (NEEC) mechanism is considered to be one of the most effective ways to excite nuclear isomers. Despite being proposed over 50 years ago, direct experimental evidence of NEEC is yet elusive. In this study, we propose an experimental scheme to examine the NEEC process using an electron beam ion trap (EBIT). In an EBIT, highly charged ions are bombarded by an electron beam, which can result in excitation of the nuclei in the trap through mechanisms such as NEEC and Coulomb excitation (CE), etc. Our calculations show that the total rates of NEEC production for some nuclei can reach over 0.1/s, which is higher than these from other mechanisms like CE. The proposed scheme may result in the confirmation of the existence of NEEC, and can also be used to study atomic nuclear excitation related processes.

KEYWORDS

nuclear excitation by electron capture, isomeric state, electron beam ion trap, highly charged ions, Coulomb excitation, production rate

1 Introduction

Nuclear isomers, being meta-stable states of nuclei, have a profound impact on various fields including nuclear structure models [1,2], nuclear astrophysics [2,3], nuclear lasers [4], nuclear batteries [5], nuclear clocks [6], fine structure measurement [7], and more [8–10]. In order to advance applications in the field of nuclear isomers, it is crucial to understand the mechanisms for exciting or de-exciting them. How to effectively excite the nucleus from the ground state to the isomeric state involves Coulomb excitation (CE) [11], photoabsorption [12], multi-photon excitation [13], and atomic processes related to electron-nucleus interaction. The latter includes nuclear excitation by electron capture (NEEC) [14], nuclear excitation by electronic transition (NEET) [15] and electron bridge (EB) [16]. Some of the more in-depth studies, such as CE and direct γ -photon absorption, their excitation probability is relatively low [17]. Therefore, the potential effective nuclear excitation mechanism of electron coupling in atoms has been considered, especially the NEEC process. NEEC is the inverse process of the internal conversion (IC). The concept of NEEC was first proposed by V.I. Goldanskii et al. in 1976 [14,17]. The principle of NEEC is shown in [Figure 1A](#). Similar to the excitation of atoms in dielectronic recombination [18], where an ion captures a free electron leading to the excitation of the atom, the NEEC is a process in which an ion captures a free electron leading to the resonance excitation of atomic nuclei, which can then be de-excited by emitting γ -ray or IC electrons. For most nuclei, their NEEC resonance cross sections are much larger than the direct photon absorption cross sections, which makes the NEEC to be a promising mechanism for effective nuclear



excitation [17]. Just like the “electron captured on nuclei” process [19,20], the NEEC process, which is an “electron captured on atoms” process, play a significant role in the nucleosynthesis in astrophysical environments [21–24], such as in stars like the sun, nova, or supernova explosions.

Considerable effort has been devoted to describing the NEEC process theoretically, as well as verifying it experimentally, which include methods of using laser-generated plasma [14,25–30], storage ring [17,31,32], channeling through crystals [33], beam-based scenario [34–36], and so on. In 2018, C. J. Chiara et al. claimed to have discovered the first experimental evidence of NEEC in the isomer depletion of ^{93m}Mo in a beam-based scenario [34]. However, this result was quickly called into questions by subsequent literature for overestimating the theoretical NEEC cross section [35,37] and underestimating the experimental backgrounds [38]. Recently, the isomer beam experiment overturned the previous experimental results [39], but the estimates of the upper limits of their yields remain consistent with the results of theoretical calculations [35,37]. Consequently, the urgent need for experimental confirmation of the NEEC process persists to this day.

In this work, we propose a new experimental scheme for verifying the existence of the NEEC process based on electron beam ion traps (EBIT). The EBIT is a type of ion trap that uses electron beams to trap and confine ions. Traditionally, the EBIT has been used in various fields, from basic atomic and molecular physics to plasma physics [40,41]. By adding an extra electron gun, the modified EBIT is expected to be used to study the nuclear physical processes like the NEEC.

The remaining sections are organized as follows: Section 2 focuses on the theoretical method of calculating the NEEC cross sections for charged ions [31,36,42]. To detect the NEEC process, Section 3 proposes an experimental setup based on an EBIT. The

numerical simulation results are provided in Section 4, demonstrating the possibility of NEEC detection. Section 5 presents a potential error budget based on the proposed experimental setup. Lastly, Section 6 provides a summary of this study.

2 NEEC resonance strengths for highly charged ions

The NEEC is a nuclear excitation process in which a free electron is captured by the atom. Its Feynman diagram is shown in Figure 1B, where the original electron e is at continuum state, and the final electron is marked as “⊙” to indicate that it is atomically bounded. By transiting the energy released from the free electron, a nuclear isomer could be produced through this process. Because of the energy conservation, one has $E_r = E_n - E_b$, where E_r is the kinetic energy carried by the free electron, E_b is the binding energy to which the free electron is captured, and E_n is the nuclear excitation energy.

It has been shown theoretically that the cross sections of the NEEC process normally are much higher than the photon absorption cross sections [31,36,42], which makes NEEC a good method to produce nuclear isomers. Furthermore, the nuclear isomer cross sections could be further enhanced if the free electron is captured to a highly charged state. In fact, as shown in Ref. [42], for a certain final electronic configuration $\alpha_r (nl_j)$ and ion charge state q before the electron capture, the NEEC cross section for a nucleus in its ground state initially is written as,

$$\sigma_{\text{NEEC}}^{q,\alpha_r}(E_e) = K \frac{\lambda_e^2}{2} \alpha_{\text{IC}}^{q,\alpha_r} \Gamma_r L_r (E_e - E_r), \quad (1)$$

where

$$K = \frac{(2J_E + 1)(2j_c + 1)}{(2J_G + 1)(2j_f + 1)}, \quad (2)$$

J_E and J_G are the nuclear spins of the excited and ground states, respectively; j_c and j_f are the total angular momenta of the captured and free electrons, respectively [22]. λ_e is the free electron wavelength, and Γ_r is the nuclear transition width of the electromagnetic radiation. The partial IC coefficients ($\alpha_{\text{IC}}^{q,\alpha_r}$), depends on the α_r and q . $L_r (E_e - E_r)$ is a Lorentzian function centered at the resonance energy E_r . The integral of the NEEC cross section $\sigma_{\text{NEEC}}^{q,\alpha_r}(E_e)$ over the free projectile electron energy E_e is called resonance strength $S_{\text{NEEC}}^{q,\alpha_r}$, which can be expressed as

$$S_{\text{NEEC}}^{q,\alpha_r} = \int \sigma_{\text{NEEC}}^{q,\alpha_r}(E_e) dE_e = K \frac{\lambda_e^2}{2} \alpha_{\text{IC}}^{q,\alpha_r} \Gamma_r. \quad (3)$$

Assuming a linear scaling dependence, one can deduce the ICCs for ionized atoms ($\alpha_{\text{IC}}^{q,\alpha_r}$) in Eq. 3 from the ICCs of neutral atoms $\alpha_{\text{IC}}^{q=0,nl_j}$ [36],

$$\alpha_{\text{IC}}^{q,\alpha_r} = \alpha_{\text{IC}}^{q=0,nl_j} \left(\frac{E_b^{q,\alpha_r}}{E_b^{q=0,nl_j}} \right) \left(\frac{n_h}{n_{\text{max}}} \right), \quad (4)$$

where E_b^{q,α_r} and $E_b^{q=0,nl_j}$ are the binding energies for ions in the charge state q and neutral atoms, respectively. Their ratio accounts for the increase of the ICCs with the ionization level [24,43]. The ratio between the present n_h and the maximum n_{max} number of

TABLE 1 The NEEC resonance strengths S for several selected heavy HCIs. The first column in the table represents the species of highly charged ions. The second ($T_{1/2}^{gs}$) and third columns ($T_{1/2}^{ex}$) are the half-lives of the ground state and isomeric state, respectively. The fourth column (E_n) lists the transition energy of the isomeric state. The 5th column is the electromagnetic transition type. The n_l represents the quantum state of the subshell where electron capture occurs. The E_r in the 8th column represents the resonant electron beam energy corresponding to NEEC. The Γ_n^{th} represents the width of the level of the isomeric state obtained via theoretical calculations. The S_{NEEC} is the resonance strength of NEEC.

HCI	$T_{1/2}^{gs}$	$T_{1/2}^{ex}$	E_n (keV)	Transition type	Subshell	n_l	E_r (keV)	Γ_n^{th} (eV)	S_{NEEC} (b-eV)
$^{154}\text{Eu}^{63+}$	8.601 y	2.2 μs	68.1702	$E1$	K	$1s_{1/2}$	11.050	2.07×10^{-10}	1.73×10^{-4}
$^{157}\text{Gd}^{64+}$	Stable	0.46 μs	63.916	$E1$	K	$1s_{1/2}$	4.850	4.62×10^{-10}	2.04×10^{-3}
$^{161}\text{Dy}^{64+}$	Stable	29.1 ns	25.65136	$E1$	L_1	$2s_{1/2}$	10.423	9.19×10^{-9}	1.46×10^{-2}
$^{181}\text{Ta}^{59+}$	Stable	6.05 μs	6.237	$E1$	M_3	$3p_{3/2}$	0.330	3.27×10^{-11}	4.34×10^{-3}
$^{231}\text{Pa}^{89+}$	3.257×10^4 y	45.1 ns	84.2152	$E1$	L_1	$2s_{1/2}$	52.244	8.03×10^{-10}	5.34×10^{-5}
$^{237}\text{Np}^{91+}$	2.144×10^6 y	67.2 ns	59.54092	$E1$	L_1	$2s_{1/2}$	25.819	3.68×10^{-9}	5.53×10^{-4}
$^{63}\text{Ni}^{28+}$	101.2 y	1.67 μs	87.15	$E2$	K	$1s_{1/2}$	76.375	2.70×10^{-10}	1.66×10^{-4}
$^{67}\text{Zn}^{30+}$	Stable	9.07 μs	93.312	$E2$	K	$1s_{1/2}$	80.923	4.91×10^{-11}	2.92×10^{-6}
$^{73}\text{Ge}^{26+}$	Stable	2.91 μs	13.2845	$E2$	L_3	$2p_{3/2}$	10.710	1.57×10^{-10}	4.23×10^{-4}
$^{83}\text{Kr}^{30+}$	Stable	156.8 ns	9.4057	$E2$	L_3	$2p_{3/2}$	6.026	2.02×10^{-10}	1.76×10^{-3}
$^{99}\text{Ru}^{44+}$	Stable	20.5 ns	89.57	$E2$	K	$1s_{1/2}$	62.536	1.86×10^{-8}	3.51×10^{-3}
$^{107}\text{Pd}^{46+}$	6.5×10^5 y	0.85 μs	115.74	$E2$	K	$1s_{1/2}$	86.117	5.36×10^{-10}	2.51×10^{-5}
$^{111}\text{Cd}^{48+}$	Stable	84.5 ns	245.390	$E2$	K	$1s_{1/2}$	213.048	5.36×10^{-9}	1.14×10^{-4}
$^{129}\text{I}^{47+}$	1.57×10^7 y	16.8 ns	27.793	$E2$	L_3	$2p_{3/2}$	19.749	2.93×10^{-9}	5.41×10^{-3}
$^{138}\text{La}^{56+}$	1.03×10^{11} y	116 ns	72.57	$E2$	K	$1s_{1/2}$	26.324	3.93×10^{-9}	1.36×10^{-3}
$^{145}\text{Nd}^{60+}$	Stable	29.4 ns	67.167	$E2$	K	$1s_{1/2}$	15.651	1.55×10^{-8}	5.49×10^{-3}
$^{152}\text{Eu}^{63+}$	13.517 y	0.94 μs	65.2969	$E2$	K	$1s_{1/2}$	8.176	4.32×10^{-11}	1.83×10^{-5}
$^{205}\text{Pb}^{46+}$	1.70×10^7 y	24.2 μs	2.329	$E2$	N_4	$4d_{3/2}$	0.037	1.89×10^{-11}	4.26×10^{-4}
$^{79}\text{Br}^{35+}$	Stable	4.85 s	207.61	$E3$	K	$1s_{1/2}$	190.673	9.44×10^{-17}	7.91×10^{-12}
$^{103}\text{Rh}^{45+}$	Stable	56.114 m	39.753	$E3$	K	$1s_{1/2}$	11.441	1.30×10^{-19}	1.59×10^{-13}
$^{107}\text{Ag}^{47+}$	Stable	44.3 s	93.125	$E3$	K	$1s_{1/2}$	62.159	1.02×10^{-17}	9.89×10^{-12}
$^{189}\text{Os}^{70+}$	Stable	5.81 h	30.82	$E4$	L_3	$2p_{3/2}$	13.200	4.54×10^{-22}	2.37×10^{-15}
$^{57}\text{Fe}^{26+}$	Stable	98.3 ns	14.4129	$M1$	K	$1s_{1/2}$	5.135	4.62×10^{-9}	5.63×10^{-2}
$^{119}\text{Sn}^{48+}$	Stable	18.03 ns	23.871	$M1$	L_1	$2s_{1/2}$	15.564	2.56×10^{-8}	1.11×10^{-1}
$^{137}\text{La}^{53+}$	6×10^4 y	89 ns	10.59	$M1$	L_2	$2p_{1/2}$	0.164	5.14×10^{-9}	8.19×10^{-2}
$^{201}\text{Hg}^{35+}$	Stable	81 ns	1.5648	$M1$	N_5	$4d_{5/2}$	0.016	3.63×10^{-10}	4.63×10^{-3}
$^{45}\text{Sc}^{21+}$	Stable	325.8 ms	12.40	$M2$	K	$1s_{1/2}$	6.366	1.40×10^{-15}	3.78×10^{-9}
$^{187}\text{Re}^{75+}$	4.33×10^{10} y	555.3 ns	206.2473	$M2$	K	$1s_{1/2}$	123.085	5.54×10^{-10}	1.36×10^{-4}
$^{158}\text{Tb}^{65+}$	180 y	10.70 s	110.3	$M3$	K	$1s_{1/2}$	49.250	4.31×10^{-17}	2.19×10^{-12}

holes in the capture subshell n_l accounts for the decrease of the ICCs for partially filled subshells [43,44].

The following steps are taken to calculate α_{IC}^{q,α_r} in Eq. 4. To obtain the ICCs of neutral atoms, $\alpha_{IC}^{q=0,n_l}$, the code BrIccFO package is employed [45], which employs the frozen orbital approximation to take into account the effect of the hole. The binding energies $E_b^{q=0,n_l}$ for neutral atoms are taken from tables in Ref. [46], while the ones for highly ionized atoms, E_b^{q,α_r} , are taken from the NIST database [47].

Isomeric states of nuclei with relatively low nuclear energy levels are chosen as potential candidates for searching NEEC experimentally, and their NEEC excitation resonance strengths are calculated, as listed in Table 1. It can be seen that for most of the longer-lived (> 1 ms) isomeric states, the NEEC excitation resonance strengths are relatively low, about 10^{-6} order of magnitude below, which may be due to the fact that the transition has a high multi-polarity. The $^{181}\text{Ta}^{59+}$, which has the relatively high electric transition strength among all the nuclei considered here, has a

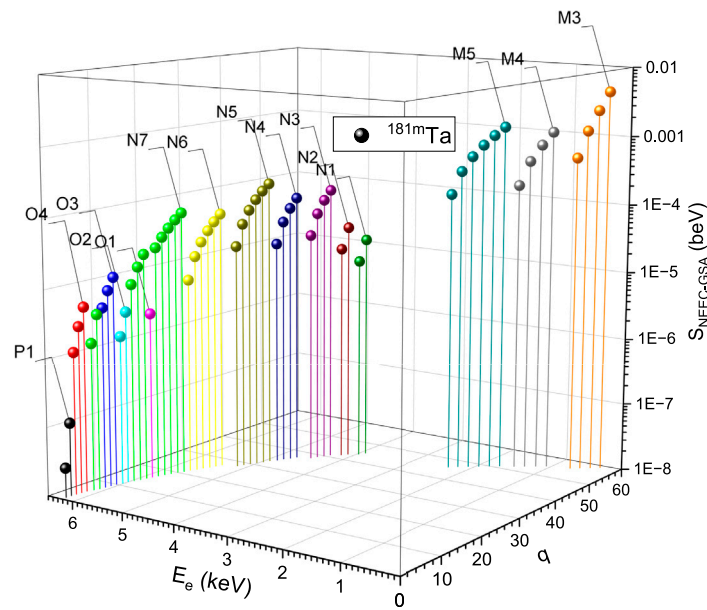


FIGURE 2

NEEC resonance strengths $S_{\text{NEEC}}^{q,\text{dr}}$ for captures into M , N , O , and P subshells as a function of the kinetic energy E_e and charge state q of $^{181\text{m}}\text{Ta}$ ions under the NEEC-GSA.

strength of 4.34×10^{-3} b-eV. It is mainly due to its very low γ transition multipolarity ($E1$), as well as its large ICC ($\alpha_{\text{IC}}^{q=0,3p_{3/2}} = 6.72$). In fact, we have conducted a detailed study of the resonance strengths of NEEC in $^{181\text{m}}\text{Ta}$ across various charged states and subshells under the ground state assumption (NEEC-GSA) [42]. Figure 2 shows resonance strengths of NEEC for $^{181\text{m}}\text{Ta}$'s M , N , O , and P subshells, calculated as a function of the projectile electron energy E_e and the charge states q ($1 \leq q \leq 59$) of $^{181\text{m}}\text{Ta}$ ions. It can be founded that the maximum value of the resonance strength is 6 orders of magnitude larger than the minimum one. The maximum resonance strength is typically observed in the inner shell, which corresponds to a higher charged state. This is due to the fact that the electrons in the inner shell are closer to the nucleus, which increases the likelihood of exciting them, as long as the energy conservation principle is satisfied.

Our calculations show that highly charged ions (HCIs), including ^{157}Gd , ^{161}Dy , ^{181}Ta , ^{83}Kr , ^{99}Ru , ^{129}I , ^{138}La , ^{145}Nd , ^{57}Fe , ^{119}Sn , ^{137}La , ^{201}Hg , etc., may be very promising in searching for the NEEC process. If they are ionized to HCIs, they are relatively easy to be excited to isomeric states due to their high NEEC resonance strengths, which are further discussed in detail in the subsequent sections.

3 Proposed experimental setup

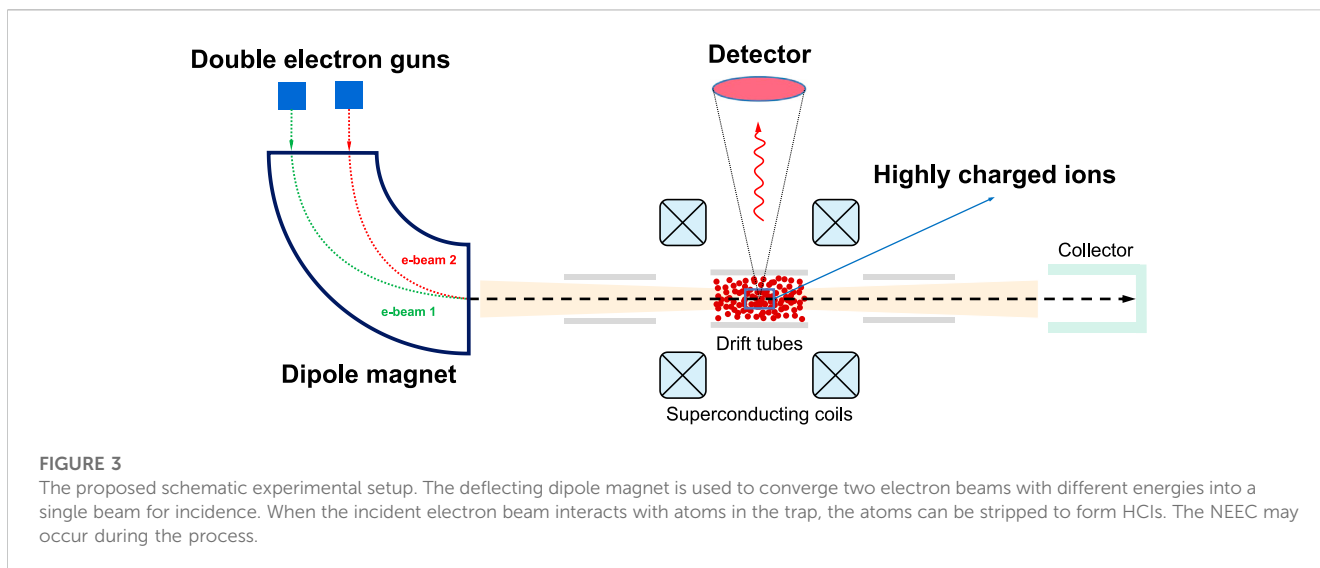
As shown in the preceding section, the calculation results indicate that the NEEC resonance strengths can be enhanced significantly if HCIs are used, suggesting their potential in NEEC search experiments. An EBIT is a device that utilizes a monoenergetic, high-current-density electron beam to generate

and then confine HCIs. With appropriate modifications, the EBITs have the potential to be valuable instruments for investigating NEEC.

The principle we propose for investigating NEEC utilizing an EBIT is illustrated in Figure 3. In contrast to conventional EBIT configurations that employ only one electron gun, our design incorporates two electron guns with varying energies. The electron beams are extracted from the electron guns and accelerated to designed energies, from tens to hundreds keV. Then the electron beams fly into the drift tubes, bombard, and then ionize the atoms there. The product ions undergo triple confinements. Firstly, they are radially confined by the spatial charge of a dense electron beam. The superconducting magnetic field provides further radial and longitudinal confinements. Further longitudinal confinement is achieved by the static electric field of three electrodes in the drift tubes. As the atoms/ions are continuously bombarded by electron beams, they can be stripped to HCIs. If the energy of the electrons matches the NEEC resonance conditions for the electron-HCI, the nuclei can be excited to their isomeric state. By placing a photon detector, such as a High-purity germanium detector, in close proximity, one can monitor the gamma photons emitted by the excited nuclei.

An electron gun can provide a beam density over 10^{13} electrons $\cdot \text{s}^{-1} \text{cm}^{-2}$, with energy fluctuation of tens of eV today. The HCIs can be confined in the trap with a diameter of tens of micrometers, a length of a few centimeters, and a density in the order of 10^8cm^{-3} . With the help of an EBIT device, HCIs of almost any element in the periodic table can now be produced.

However, the energy required for stripping does not necessarily match that for the resonance. Therefore, to address this issue, in our proposed setup, we use two electron guns. One gun is tuned to strip



the atoms to HCIs, while the other is tuned to match the resonance conditions of the NEEC. As shown in Figure 3, the two electron beams from the two electron guns can be deflected by a dipole magnet, converge to be co-axial, and then pass through the confined HCIs area. As an example, for isotope ^{181}Ta , by tuning the first electron gun to 17.721 keV, one can stripe it to $^{181}\text{Ta}^{59+}$ [48]. If tuning the second electron gun to 0.33 keV, the 0.33 keV electrons from the 2nd gun can excite $^{181}\text{Ta}^{59+}$ to their isomeric state of $(9/2^-, 6.237 \text{ keV})$ with the cross section of $4.34 \times 10^{-3} \text{ b}\cdot\text{eV}$.

4 Estimation of NEEC reaction rates

Consider HCIs that are trapped in an EBIT, as shown in Figure 3. It is assumed that the ions are confined within a cylindrical volume with a radius of R and a length of L cm. Additionally, it is assumed that the electron energy spectrum follows a Gaussian distribution with a width of ϵ_e . The spatial spreading of the electron beam is also assumed to be Gaussian with a width of σ_b . The rate of nuclear isomers generated by the NEEC process for a given electron beam in EBIT can be written using the resonance strength Eq. 3 as

$$R_{\text{NEEC}}(E_e) = \int_e^j f(E_e - E_r) n_i \sigma_{\text{NEEC}}(E_e) L dE \quad (5)$$

$$= \frac{j}{e} f(E_e - E_r) n_i S_{\text{NEEC}} L,$$

where j represents the electron beam current intensity, e is the charge of an electron, n_i represents the density of ion trapped in an EBIT, L is the length of the ion cluster in the trap, E_e is the energy of the electron beam, and $f(E_e - E_r)$ represents the energy distribution of the electron beam.

To ensure practicality, we initially screened candidate nuclei for NEEC studies based on certain criteria. Ideally, we looked for stable isotopes or isotopes with a long lifetime (more than 1 year) to avoid the need for a radioactive ion source. Additionally, we preferred isotopes with relatively lower transition energy (less than 300 keV) since it is hard for typical EBITs to provide electron energies larger

than that. We also considered the lifetime of the isomeric state, which should be relatively long but not too long (in the range of tens of nanoseconds to microseconds). A longer lifetime results in a narrower resonance width and smaller reaction yield. However, if the lifetime is too short, it may overlap with the radioactive recombination (RR) process [49,50], which is an atomic process with a short lifetime, typically in order of 10^{-14} s [49]. The RR can be a significant background for NEEC studies.

Taking ^{181}Ta as an example, it can be stripped to the 59^+ valence state, which corresponds to a binding energy of $E_b = 5.907 \text{ keV}$. To achieve the highest ratio of expected charge state to all ions, the stripping electron beam energy E_{es} should be tuned to be 2 ~ 3 times the ion binding energy E_b , i.e., $E_{es} \approx (2 \sim 3)E_b$ [48]. Ta ions can capture an electron to the $3p_{3/2}$ atomic level (58^+ charge state) through the NEEC process while being excited from the ground state ($J^\pi = 7/2^+$, stable) to a 6.237 keV isomeric state ($J^\pi = 9/2^-, T_{1/2}^{\text{ex}} = 6.05 \mu\text{s}$). Therefore, for the beam serving as the NEEC resonance beam to match the nuclear excitation resonance condition, its beam energy E_{er} can be tuned to be 0.33 keV.

Consider that ^{181}Ta ions are trapped in a typical EBIT, and the trapped ions fill a cylindrical volume with a radius of $50 \mu\text{m}$ and a length of 3 cm. We assume that n_i is 10^8 cm^{-3} in the ion trap and that a resonant electron beam with a current of 200 mA is incident. The electron beam with an energy spread of under 50 eV (ϵ_e) and a radius of about $50 \mu\text{m}$ (σ_b) is achievable today. Normally the nuclear energy level width $\Gamma_n^{\text{th}} = \Gamma_\gamma + \Gamma_{\text{IC}}$ is very narrow compared with the beam energy spread, where Γ_{IC} represents the IC decay width. For instance, the ^{181}Ta isotope's total nuclear transition width is approximately $\Gamma_n^{\text{th}} = 3.27 \times 10^{-11} \text{ eV}$, compared with the electron beam energy spread of 50 eV. Therefore, we also need to consider the influence of resonance strength. The value of the resonance strength is calculated to be $S_{\text{NEEC}} = 4.34 \times 10^{-3} \text{ b}\cdot\text{eV}$ at the resonance energy $E_r = 0.33 \text{ keV}$.

The calculated rates based on the above assumptions are listed in Table 2. As an order of magnitude estimation, the distribution of charge states is not considered. Here only one charge state is considered and other charge states are ignored. For $^{181}\text{Ta}^{59+}$, the

TABLE 2 In a typical EBIT with a length of 3 cm, the ion density n_i is assumed to be 10^8 cm^{-3} . The current of the incident electron beam with an energy broadening of 50 eV is 200 mA. The reaction rates R_{NEECCE} for NEEC and CE processes at two different electron beam energies of some HCIs in Table 1. Here the contribution to R_{NEECCE} comes from the both electron beams, E_{er} and E_{es} and $R_{\text{tot}} = R_{\text{NEEC}} + R_{\text{CE}}$.

HCIs	E_n (keV)	Transition type	E_{er} (keV)	E_{es} (keV)	$R_{\text{NEEC}} (s^{-1})$	$R_{\text{CE}} (s^{-1})$	$R_{\text{tot}} (s^{-1})$	Dominated by
$^{154}\text{Eu}^{63+}$	68.1702	E1	11.050	171.362	5.17×10^{-4}	1.33×10^{-8}	5.17×10^{-4}	NEEC
$^{157}\text{Gd}^{62+}$	63.916	E1	4.850	177.197	6.10×10^{-3}	1.56×10^{-7}	6.10×10^{-3}	NEEC
$^{161}\text{Dy}^{64+}$	25.65136	E1	10.423	45.684	4.36×10^{-2}	9.89×10^{-5}	4.37×10^{-2}	NEEC
$^{181}\text{Ta}^{59+}$	6.237	E1	0.330	17.721	1.30×10^{-2}	1.07×10^{-2}	2.36×10^{-2}	NEEC and CE
$^{237}\text{Np}^{91+}$	59.54092	E1	25.819	101.167	1.65×10^{-3}	1.55×10^{-7}	1.65×10^{-3}	NEEC
$^{63}\text{Ni}^{28+}$	87.15	E2	76.375	32.326	4.96×10^{-4}	0	4.96×10^{-4}	NEEC
$^{73}\text{Ge}^{26+}$	13.2845	E2	10.710	7.725	1.26×10^{-3}	0	1.26×10^{-3}	NEEC
$^{83}\text{Kr}^{30+}$	9.4057	E2	6.026	10.140	5.26×10^{-3}	1.95×10^{-3}	7.21×10^{-3}	NEEC and CE
$^{99}\text{Ru}^{44+}$	89.57	E2	62.536	81.101	1.05×10^{-2}	0	1.05×10^{-2}	NEEC
$^{111}\text{Cd}^{48+}$	245.390	E2	213.048	97.025	3.41×10^{-4}	0	3.41×10^{-4}	NEEC
$^{129}\text{I}^{47+}$	27.793	E2	19.749	24.132	1.62×10^{-2}	0	1.62×10^{-2}	NEEC
$^{138}\text{La}^{56+}$	72.57	E2	26.324	138.737	4.06×10^{-3}	2.76×10^{-6}	4.07×10^{-3}	NEEC
$^{145}\text{Nd}^{60+}$	67.167	E2	15.651	154.547	1.64×10^{-2}	1.50×10^{-5}	1.64×10^{-2}	NEEC
$^{205}\text{Pb}^{46+}$	2.329	E2	0.037	6.876	1.27×10^{-3}	6.74×10^{-3}	8.01×10^{-3}	NEEC and CE
$^{57}\text{Fe}^{26+}$	14.4129	M1	5.135	27.833	1.68×10^{-1}	5.43×10^{-2}	2.23×10^{-1}	NEEC and CE
$^{119}\text{Sn}^{48+}$	23.871	M1	15.564	24.921	3.32×10^{-1}	3.58×10^{-10}	3.32×10^{-1}	NEEC
$^{137}\text{La}^{53+}$	10.59	M1	0.164	31.278	2.45×10^{-1}	5.54×10^{-7}	2.45×10^{-1}	NEEC
$^{201}\text{Hg}^{35+}$	1.5648	M1	0.016	4.647	1.38×10^{-2}	1.26×10^{-2}	2.64×10^{-2}	NEEC and CE
$^{187}\text{Re}^{75+}$	1.5648	M2	123.085	249.487	4.06×10^{-4}	1.90×10^{-13}	4.06×10^{-4}	NEEC

reaction rate is $1.3 \times 10^{-2}/s$ for the electron beam with the energy of 0.33 keV, while for the beam of 17.721 keV, the reaction rate can be negligible due to the production rate being below the order of magnitude of $10^{-30}/s$. Therefore, the total reaction rate of NEEC, i.e., $R_{\text{NEEC}} = R_{\text{NEEC}}(E_{er}) + R_{\text{NEEC}}(E_{es})$, is approximately equal to $R_{\text{NEEC}}(E_{er})$.

The reaction rates of CE, i.e., $R_{\text{CE}}(E_e) = In_i\sigma_{\text{CE}}(E_e)L$, $I = j/e$, are also considered, where CE cross sections were calculated using semi-classical theory [51]. The total reaction rates of CE, i.e., $R_{\text{CE}} = R_{\text{CE}}(E_{er}) + R_{\text{CE}}(E_{es})$ are listed in Table 2 too. For the 0.33 keV beam, the energy is too low and the reaction is forbidden; for the 17.721 keV beam, the CE rate and the NEEC rate are in the same order of $10^{-2}/s$. This nucleus has a relatively high isomer generation rate $R_{\text{tot}} = R_{\text{CE}} + R_{\text{NEEC}}$ in all the nuclei considered in this work. Indeed, some nuclei, such as ^{57}Fe , ^{119}Sn , and ^{137}La , can be produced at rates greater than 0.1/s.

For other HCIs considered in this work, such as $^{154}\text{Eu}^{63+}$, $^{157}\text{Gd}^{62+}$, $^{237}\text{Np}^{91+}$, $^{63}\text{Ni}^{28+}$, $^{111}\text{Cd}^{48+}$, $^{119}\text{Sn}^{48+}$, $^{137}\text{La}^{53+}$, and $^{187}\text{Re}^{75+}$, their NEEC excitation rates are much greater than the CE, which is very beneficial to prove the existence of the NEEC process. In particular, for $^{63}\text{Ni}^{28+}$, $^{73}\text{Ge}^{26+}$, $^{99}\text{Ru}^{44+}$, $^{111}\text{Cd}^{48+}$, and $^{129}\text{I}^{47+}$ ions, the resonant and stripping electron beam energies are both less than the nuclear excitation energy. This means that the CE excitation is energetically forbidden, and only the NEEC excitation is present.

5 Discussion

The decay of the isomers [52] are mainly through gamma transition and IC (collectively referred to as isomeric transition or IT decay); partly through beta decay such as β^- , β^+ , orbital electron capture on nuclei; and a small amount through alpha decay, neutron emission, neutrino-nucleus processes, etc. However, all of our selected nuclei are stable, and their excited state decay is only IT decay.

The major backgrounds for NEEC searching come from RR and CE processes [50,53,54]. However, it should be noted that the NEEC is a resonance process, while CE processes are not resonance processes. This difference in resonance properties allows for the possibility of distinguishing the resonance peak from the flat background in the NEEC search. We have calculated the excitation rates of the possible CE and NEEC processes for different HCIs separately, as an example shown in Table 2. For most cases where both the electron beams are taken into account and the energies of the beams are smaller than 300 keV, cross sections due to CE are much smaller than the corresponding NEEC process cross sections.

The search for NEEC faces significant interference from the RR process, which is another major background. However, as a broad-resonant process, the RR process has anisotropic angular

distributions [50], whereas the distribution of NEEC is isotropic. The combination of an isotropic distribution and a resonance peak can help distinguish the NEEC from the RR process. In addition, since the selected isomers are long-lived, they can be extracted from the ion trap to a clean environment for observation like [39,54] to avoid the interference of other background processes.

There may be competition between the NEEC and stripping processes. The former process involves adding an electron to a HCl, while the latter involves removing one. However, the time scale of nuclear excitation process is much shorter than the time scale required to strip electrons from outside the nucleus at high energies [55,56]. Therefore, the interference between the two processes can be negligible.

The expected thermal motion of ions in the trap is in the order of < 10 eV, which is smaller than the energy spread of the resonance electron beam at around 50 eV. As a result, the Doppler effect resulting from the ions' thermal motion in the trap can be considered negligible [57]. Furthermore, other factors may cause changes in nuclear energy levels and their widths, such as the confinement magnet. The Zeeman effect causes energy levels of nuclei and atoms to split, with the energy splits ($\Delta E \propto B$) typically being small due to limited confinement magnetic fields [58]. Therefore, given the electron beam's energy spread of about 50 eV, the Zeeman effect can also be considered negligible.

Based on the estimated NEEC rates listed in Table 2 which are practically measurable and the controllable background noise signals discussed above, it is promising to search for the NEEC process using the proposed setup.

6 Summary

In summary, we propose an experimental scheme to study NEEC by utilizing an EBIT with two electron beams. The first electron beam strips atoms in the EBIT to high charge states, while the second electron beam matches the energy required for the NEEC process. Our calculations show that this approach yields high cross sections and sufficient reaction products. A resonance strength in the order of magnitude of 10^{-3} b-eV is achievable by using nuclei like $^{181}\text{Ta}^{59+}$, $^{137}\text{La}^{53+}$, $^{119}\text{Sn}^{48+}$, etc. The proposed scheme can be implemented with minimal modifications to existing EBIT setups, requiring only an additional electron gun and photon detectors. We are confident that our proposed scheme will stimulate additional research on NEEC processes and potentially confirm the existence of this phenomenon, which has been extensively investigated for over 50 years but has yet to be confirmed. Furthermore, we anticipate that

our proposed scheme could be adapted to investigate other exotic processes (e.g., the NEET or EB process after further modifications) and potentially contribute to further advances in our understanding of nuclear physics.

Data availability statement

The original contributions presented in the study are included in the article/supplementary material, further inquiries can be directed to the corresponding authors.

Author contributions

This study was proposed by CF, WH, and YM. The theoretical calculations in this manuscript were done by YW under the guidance of CF and also discussed the theory of NEEC with YY, ZM, and WH. ZM and CF provided theoretical support on the CE. The initial draft of this manuscript was written by YW and further revised by CF. All authors contributed to the article and approved the submitted version.

Funding

This work is supported by the National Natural Science Foundation of China (NSFC) under Grant No. 12235003.

Conflict of interest

The authors declare that the research was conducted in the absence of any commercial or financial relationships that could be construed as a potential conflict of interest.

Publisher's note

All claims expressed in this article are solely those of the authors and do not necessarily represent those of their affiliated organizations, or those of the publisher, the editors and the reviewers. Any product that may be evaluated in this article, or claim that may be made by its manufacturer, is not guaranteed or endorsed by the publisher.

References

1. Dracoulis GD, Walker PM, Kondev FG. Review of metastable states in heavy nuclei. *Rep Prog Phys* (2016) 79:076301. doi:10.1088/0034-4885/79/7/076301
2. Walker P, Dracoulis G. Energy traps in atomic nuclei. *Nature* (1999) 399:35–40. doi:10.1038/19911
3. Belic D, Arlandini C, Besserer J, De Boer J, Carroll J, Enders J, et al. Photoactivation of ^{180}Ta and its implications for the nucleosynthesis of nature's rarest naturally occurring isotope. *Phys Rev Lett* (1999) 83:5242–5. doi:10.1103/physrevlett.83.5242
4. Tkalya E. Proposal for a nuclear gamma-ray laser of optical range. *Phys Rev Lett* (2011) 106:162501. doi:10.1103/physrevlett.106.162501
5. Carroll JJ. Nuclear structure and the search for induced energy release from isomers. *Nucl Instr Methods Phys Res Section B: Beam Interactions Mater Atoms* (2007) 261:960–4. doi:10.1016/j.nimb.2007.04.128
6. von der Wense L, Seiferle B. The ^{229}Th isomer: Prospects for a nuclear optical clock. *The Eur Phys J A* (2020) 56:277. doi:10.1140/epja/s10050-020-00263-0
7. Flambaum VV. Enhanced effect of temporal variation of the fine structure constant and the strong interaction in ^{229}Th . *Phys Rev Lett* (2006) 97:092502. doi:10.1103/PhysRevLett.97.092502
8. Banerjee S, Ambikalmajan Pillai MR, Ramamoorthy N. Evolution of ^{99m}Tc in diagnostic radiopharmaceuticals. *Semin Nucl Med* (2001) 31:260–77. doi:10.1053/snuc.2001.26205

9. Zhang ZZ, Wang HL, Meng HY, Liu ML. Uncertainty evaluation and correlation analysis of single-particle energies in phenomenological nuclear mean field: An investigation into propagating uncertainties for independent model parameters. *Nucl Sci Tech* (2021) 32:16. doi:10.1007/s41365-021-00851-9
10. Ma Z, Fu C, He W, Ma Y. Manipulation of nuclear isomers with lasers: Mechanisms and prospects. *Sci Bull* (2022) 67:1526–9. doi:10.1016/j.scib.2022.06.020
11. Hayes AB, Cline D, Wu CY, Ai J, Amro H, Beausang C, et al. Breakdown of k selection in ^{178}Hf . *Phys Rev Lett* (2006) 96:042505. doi:10.1103/PhysRevLett.96.042505
12. Collins CB, Davanloo F, Isosif MC, Dussart R, Hicks JM, Karamian SA, et al. Accelerated emission of gamma rays from the 31-yr isomer of ^{178}Hf induced by x-ray irradiation. *Phys Rev Lett* (1999) 82:695–8. doi:10.1103/PhysRevLett.82.695
13. Tkalya E. Many-photon excitation of atomic nuclei in the hot plasma. *Soviet Phys Doklady* (1991) 36:467.
14. Goldanskii VI, Namiot VA. On the excitation of isomeric nuclear levels by laser radiation through inverse internal electron conversion. *Phys Lett B* (1976) 62:393–4. doi:10.1016/0370-2693(76)90665-1
15. Kishimoto S, Yoda Y, Seto M, Kobayashi Y, Kitao S, Haruki R, et al. Observation of nuclear excitation by electron transition in ^{197}Au with synchrotron x rays and an avalanche photodiode. *Phys Rev Lett* (2000) 85:1831–4. doi:10.1103/PhysRevLett.85.1831
16. Bilous PV, Bekker H, Berengut JC, Seiferle B, von der Wense L, Thirolf PG, et al. Electronic bridge excitation in highly charged ^{229}Th ions. *Phys Rev Lett* (2020) 124:192502. doi:10.1103/PhysRevLett.124.192502
17. Pálffy A, Evers J, Keitel CH. Isomer triggering via nuclear excitation by electron capture. *Phys Rev Lett* (2007) 99:172502. doi:10.1103/PhysRevLett.99.172502
18. Harman Z, Shah C, González Martínez AJ, Jentschura UD, Tawara H, Keitel CH, et al. Resonance strengths for kl dielectronic recombination of highly charged mercury ions and improved empirical z -scaling law. *Phys Rev A* (2019) 99:012506. doi:10.1103/PhysRevA.99.012506
19. Giannaka P, Kosmas T, Ejiri H. Original e^- Capture Cross Sections for Hot Stellar Interior Energies. *Particles* (2022) 5:390–406. doi:10.3390/particles5030031
20. Langanke K, Martínez-Pinedo G, Zegers RGT. Electron capture in stars. *Rep Prog Phys* (2021) 84:066301. doi:10.1088/1361-6633/abf207
21. Helmrich S, Spennberg K, Pálffy A. Coupling highly excited nuclei to the atomic shell in dense astrophysical plasmas. *Phys Rev C* (2014) 90:015802. doi:10.1103/PhysRevC.90.015802
22. Harston MR, Chemin JF. Mechanisms of nuclear excitation in plasmas. *Phys Rev C* (1999) 59:2462–73. doi:10.1103/PhysRevC.59.2462
23. Gosselin G, Méot V, Morel P. Modified nuclear level lifetime in hot dense plasmas. *Phys Rev C* (2007) 76:044611. doi:10.1103/PhysRevC.76.044611
24. Gosselin G, Morel P. Enhanced nuclear level decay in hot dense plasmas. *Phys Rev C* (2004) 70:064603. doi:10.1103/PhysRevC.70.064603
25. Gunst J, Litvinov YA, Keitel CH, Pálffy A. Dominant secondary nuclear photoexcitation with the x-ray free-electron laser. *Phys Rev Lett* (2014) 112:082501. doi:10.1103/PhysRevLett.112.082501
26. Wu Y, Gunst J, Keitel CH, Pálffy A. Tailoring laser-generated plasmas for efficient nuclear excitation by electron capture. *Phys Rev Lett* (2018) 120:052504. doi:10.1103/PhysRevLett.120.052504
27. Wu D, Bai CL, Sagawa H, Song ZQ, Zhang HQ. Contributions of optimized tensor interactions on the binding energies of nuclei. *Nucl Sci Tech* (2020) 31:14. doi:10.1007/s41365-020-0727-7
28. He YF, Sun B, Ma MJ, Li W, He QY, Cui ZH, et al. Topology optimization of on-chip integrated laser-driven particle accelerator. *Nucl Sci Tech* (2022) 33:120. doi:10.1007/s41365-022-01101-2
29. Lan HY, Wu D, Liu JX, Zhang JY, Lu HG, Lv JF, et al. Photonuclear production of nuclear isomers using bremsstrahlung induced by laser-wakefield electrons. *Nucl Sci Tech* (2023) 34:74. doi:10.1007/s41365-023-01219-x
30. Hu P, Ma ZG, Zhao K, Zhang GQ, Fang DQ, Wei BR, et al. Development of gated fiber detectors for laser-induced strong electromagnetic pulse environments. *Nucl Sci Tech* (2021) 32:58. doi:10.1007/s41365-021-00898-8
31. Pálffy A, Scheid W, Harman Z. Theory of nuclear excitation by electron capture for heavy ions. *Phys Rev A* (2006) 73:012715. doi:10.1103/PhysRevA.73.012715
32. Ma X, Wen WQ, Huang ZK, Wang HB, Yuan YJ, Wang M, et al. Proposal for precision determination of 7.8 eV isomeric state in ^{229}Th at heavy ion storage ring. *Physica Scripta* (2015) T166:014012. doi:10.1088/0031-8949/2015/T166/014012
33. Yuan ZS, Kimball JC. First-principles calculation of the cross sections for nuclear excitation by electron capture of channeled nuclei. *Phys Rev C* (1993) 47:323–8. doi:10.1103/PhysRevC.47.323
34. Chiara C, Carroll J, Carpenter M, Greene J, Hartley D, Janssens R, et al. Isomer depletion as experimental evidence of nuclear excitation by electron capture. *Nature* (2018) 554:216–8. doi:10.1038/nature25483
35. Wu Y, Keitel CH, Pálffy A. ^{93m}Mo isomer depletion via beam-based nuclear excitation by electron capture. *Phys Rev Lett* (2019) 122:212501. doi:10.1103/PhysRevLett.122.212501
36. Rzadkiewicz J, Polasik M, Ślabkowska K, Syrocki L, Węder E, Carroll JJ, et al. Beam-based scenario for ^{242m}Am isomer depletion via nuclear excitation by electron capture. *Phys Rev C* (2019) 99:044309. doi:10.1103/PhysRevC.99.044309
37. Rzadkiewicz J, Polasik M, Ślabkowska K, Syrocki L, Carroll JJ, Chiara CJ. Novel approach to ^{93m}Mo isomer depletion: Nuclear excitation by electron capture in resonant transfer process. *Phys Rev Lett* (2021) 127:042501. doi:10.1103/PhysRevLett.127.042501
38. Guo S, Fang Y, Zhou X, Petrache C. Possible overestimation of isomer depletion due to contamination. *Nature* (2021) 594:E1–2. doi:10.1038/s41586-021-03333-5
39. Guo S, Ding B, Zhou XH, Wu YB, Wang JG, Xu SW, et al. Probing ^{93m}Mo isomer depletion with an isomer beam. *Phys Rev Lett* (2022) 128:242502. doi:10.1103/PhysRevLett.128.242502
40. Currell F, Fussmann G. Physics of electron beam ion traps and sources. *IEEE Trans Plasma Sci* (2005) 33:1763–77. doi:10.1109/TPS.2005.860072
41. Lapiere A, Crespo López-Urrutia JR, Braun J, Brenner G, Bruhns H, Fischer D, et al. Lifetime measurement of the $ar_{xiv} \{1\}\{2\}2\{s\}\{2\}2p\{phantom\{\rule{0.2em}{0ex}\}\{2\}p_{-3/2}\{o\}$ metastable level at the heidelberg electron-beam ion trap. *Phys Rev A* (2006) 73:052507. doi:10.1103/PhysRevA.73.052507
42. Gargiulo S, Madan I, Carbone F. Nuclear excitation by electron capture in excited ions. *Phys Rev Lett* (2022) 128:212502. doi:10.1103/PhysRevLett.128.212502
43. Rysav M, Dragoun O. On the reliability of the theoretical internal conversion coefficients. *J Phys G: Nucl Part Phys* (2000) 26:1859–72. doi:10.1088/0954-3899/26/12/309
44. Raman S, Nestor CW, Ichihara A, Trzhaskovskaya MB. How good are the internal conversion coefficients now? *Phys Rev C* (2002) 66:044312. doi:10.1103/PhysRevC.66.044312
45. Kibédi T, Burrows T, Trzhaskovskaya M, Davidson P, Nestor C. Evaluation of theoretical conversion coefficients using bricc. *Nucl Instr Methods Phys Res Section A: Acc Spectrometers, Detectors Associated Equipment* (2008) 589:202–29. doi:10.1016/j.nima.2008.02.051
46. Larkins F. Semiempirical auger-electron energies for elements 10 - z - 100. *At Data Nucl Data Tables* (1977) 20:311–87. doi:10.1016/0092-640X(77)90024-9
47. [Dataset] Kramida A, Ralchenko Y, Reader J. *NAT. Nist atomic spectra database*. version 5.10 (2022). doi:10.18434/T4W30F
48. Pálffy A. *Theory of nuclear excitation by electron capture for heavy ions*. Germany: Justus-Liebig-University Giessen (2006). Ph.D. thesis.
49. Pálffy A, Harman Z, Kozhuharov C, Brandau C, Keitel CH, Scheid W, et al. Nuclear excitation by electron capture followed by fast x-ray emission. *Phys Lett B* (2008) 661:330–4. doi:10.1016/j.physletb.2008.02.027
50. Pálffy A, Harman Z, Scheid W. Quantum interference between nuclear excitation by electron capture and radiative recombination. *Phys Rev A* (2007) 75:012709. doi:10.1103/PhysRevA.75.012709
51. Alder K, Bohr A, Huus T, Mottelson B, Winther A. Study of nuclear structure by electromagnetic excitation with accelerated ions. *Rev Mod Phys* (1956) 28:432–542. doi:10.1103/revmodphys.28.432
52. Sagawa AO. *Modern nuclear physics*. Singapore: Springer (2021).
53. Arigapudi SK, Pálffy A. Overlapping resonances in nuclei coupling to the atomic shells. *Phys Rev A* (2012) 85:012710. doi:10.1103/PhysRevA.85.012710
54. Feng J, Wang W, Fu C, Chen L, Tan J, Li Y, et al. Femtosecond pumping of nuclear isomeric states by the coulomb collision of ions with quivering electrons. *Phys Rev Lett* (2022) 128:052501. doi:10.1103/PhysRevLett.128.052501
55. Shang JJS. Modeling plasma via electron impact ionization. *Aerospace* (2018) 5:2. doi:10.3390/aerospace5010002
56. Jonaskas V, Kynienė A, Kučas S, Pakalka S, Ivč M, Pranciševičius A, et al. Electron-impact ionization of w^{5+} . *Phys Rev A* (2019) 100:062701. doi:10.1103/PhysRevA.100.062701
57. Beiersdorfer P, Phillips TW, Wong KL, Marrs RE, Vogel DA. Measurement of level-specific dielectronic-recombination cross sections of heliumlike Fe XXV. *Phys Rev A* (1992) 46:3812–20. doi:10.1103/PhysRevA.46.3812
58. Zou Y, Hutton R. Physics based on electron beam ion traps*. *Physica Scripta* (2005) T120:47–52. doi:10.1088/0031-8949/2005/T120/006